Fabrication of Ni–B alloy coated vapor-grown carbon nanofibers by electroless deposition

Susumu Arai, Yuzo Imoto, Yosuke Suzuki, Morinobu Endo

PII: S0008-6223(10)00898-5
DOI: 10.1016/j.carbon.2010.12.019
Reference: CARBON 6282

To appear in: *Carbon*

Received Date: 9 September 2010
Accepted Date: 6 December 2010

Please cite this article as: Arai, S., Imoto, Y., Suzuki, Y., Endo, M., Fabrication of Ni–B alloy coated vapor-grown carbon nanofibers by electroless deposition, *Carbon* (2010), doi: 10.1016/j.carbon.2010.12.019

Fabrication of Ni–B alloy coated vapor-grown carbon nanofibers by electroless deposition

Susumu Arai[a,*] , Yuzo Imoto[a], Yosuke Suzuki[a], Morinobu Endo[b]

[a] Department of Chemistry and Material Engineering, Faculty of Engineering, Shinshu University, 4-17-1 Wakasato, Nagano-shi, Nagano 380-8553, Japan

[b] Department of Electrical and Electronic Engineering, Faculty of Engineering, Shinshu University, 4-17-1 Wakasato, Nagano-shi, Nagano 380-8553, Japan

*Corresponding author. Fax: +81 26 269 5432. E-mail address: araisun@shinshu-u.ac.jp (S. Arai)

Abstract

Ni–B alloy coated vapor-grown carbon nanofibers (VGCNFs) were fabricated by electroless deposition and their microstructures were investigated. The effects of heat treatment on the coated VGCNFs were also studied. VGCNFs could be coated with a homogeneous Ni–B alloy film using a plating bath containing dimethylaminoborane (DMAB) as a reducing agent. The boron content of the Ni–B alloy film could be varied from 14 to 24 atom% B by varying the DMAB concentration of the plating bath. The VGCNFs were uniformly coated with a Ni–B alloy layer that was only several nanometers thick. The coating thickness on the VGCNFs could be controlled by varying the reaction time. The Ni–B alloy coatings formed in this study were semicrystalline or amorphous depending on the boron content of the alloy film. After heat treatment, the phase structure of the Ni–B alloy coatings changed to a stable crystalline structure consisting of a face-centered-cubic nickel phase and a Ni_3B phase. No cracks or exfoliation of the coatings were observed, even after heat treatment.

1. Introduction

Carbon nanotubes (CNTs) [1,2] and vapor-grown carbon nanofibers (VGCNFs) have excellent mechanical characteristics including high tensile strength and high elastic modulus. Research into practical applications of CNTs and VGCNFs, including the preparation of resin/CNT or VGCNFs, ceramic/CNT or VGCNFs, and metal/CNT or VGCNFs composites, has been actively pursued. When fabricating CNT or VGCNFs composites, the wettability of the CNTs or VGCNFs and the matrix material is very important. Since CNTs also have electromagnetic wave shielding properties, the use of CNT composites materials for electromagnetic wave shielding has been investigated [3,4]. Furthermore, as CNTs and VGCNFs have superior chemical and physical inertness and large specific surfaces, they are expected to be potential supports for catalysts, such as fuel cell electrode catalysts [5,6]. Metal coatings or deposition on CNTs [7,8] or VGCNFs is considered to be effective for improving their wettability with the matrix of composites; it could also be useful for fabricating novel catalysts that use CNTs or VGCNFs as the support. Ferromagnetic metallic coatings such as cobalt coatings on CNTs or VGCNFs are expected to make CNTs or VGCNFs ferromagnetic and enhance the electromagnetic wave shielding properties of composites containing them.

Electroless Ni–B alloy coatings have been used as protecting films for mechanical components due to their high hardness and wear resistance [9–16]. Electroless Ni–B alloy coatings have also been used to facilitate sintering of hard particles such as WC, VC [17], B_4C [18,19], and diamond [20] particles. Recently, electroless Ni–B alloy coatings have also been applied to electromagnetic wave shielding [21]. Electroless Ni–B alloy coatings, especially amorphous Ni–B alloy coatings or deposits, have been examined as catalysts for hydrogenation reactions [22–27].

Electroless Ni–B alloy coated CNTs or VGCNFs are thus considered to be promising materials for various applications. However, fabrication of electroless Ni–B alloy coated or deposited CNTs and/or VGCNFs has not been reported. In this study, we investigated Ni–B alloy coatings on VGCNFs by electroless deposition and evaluated the effects of heat treatment on the Ni–B alloy coated VGCNFs.

2. Experimental

2.1 Chemicals

Commercially available VGCNFs (VGCFs, Showa Denko Co. Ltd.) were used in the present study. The VGCFs had a diameter of 150 nm and a length of 10 μm. The VGCFs are graphitized VGCNFs that had been heat treated at 2800°C in argon gas for 30 min [28]. $NiSO_4 \cdot 6H_2O$, $C_6H_5Na_3O_7 \cdot 2H_2O$, dimethylaminoborane (DMAB), $SnCl_2 \cdot H_2O$, and $PdCl_2$ (Wako Pure Chemical Industries, Ltd.) were used in this study; they are special-grade reagents. First-grade polyacrylic acid with a mean molecular weight of 5000 (PA-5000, Wako Pure Chemical Industries, Ltd.) was used to disperse the VGCNFs. Pure water from an electrodialysis water purifier (RFP343RA, Advantec MFS, Inc.) was used in all experiments.

2.2 Sensitization and activation of the VGCNFs

Since VGCNFs are hydrophobic, the VGCNFs were first dispersed in an aqueous solution of PA-5000 that was agitated using a stirrer and ultrasonic irradiation. After dispersion, the

VGCNFs were filtered and added to a 4.4×10^{-2} M $SnCl_2{\cdot}2H_2O$ + 0.12 M HCl solution at 25 °C with agitation (ultrasonic irradiation: 1 min, stirrer agitation: 5 min) to absorb Sn^{2+} ions on the VGCNFs (sensitization). After filtering, the VGCNFs were then immersed in a 5.6×10^{-4} M $PdCl_2$ + 0.12 M HCl solution at 25°C with agitation (ultrasonic irradiation: 1 min, stirrer agitation: 5 min) to form palladium catalytic nuclei on the VGCNFs (activation).

2.3 Electroless Ni–B alloy deposition on VGCNFs

After activation, the VGCNFs were placed in electroless plating baths for Ni–B alloy deposition. The electroless plating bath composition used was 0.1 M $NiSO_4{\cdot}6H_2O$ + 0.1 M $Na_3C_6H_5O_7$ + x M DMAB. The bath pH was varied from 4 to 10. Electroless plating was performed with stirrer agitation at 30°C.

2.4 Heat-treatment of Ni–B alloy deposited VGCNFs

The Ni–B alloy coated VGCNFs were heated at various temperatures for 1 h in an infrared heating furnace (mini lamp annealer; MILA-3000, Ulvac-Riko Inc.) in vacuum.

2.5 Characterization of electroless Ni–B alloy deposits on VGCNFs

The Ni–B alloy deposits on the VGCNFs were observed by field-emission scanning electron microscopy (SEM; JSM-7000F, Jeol and SU-8000, Hitachi) and scanning transmission electron microscopy (STEM; HD-2300A, Hitachi). The phase structures of the deposits were analyzed by

X-ray diffraction (XRD) using Cu $K\alpha_1$ radiation (XRD-6000, Shimadzu Seisakusho). The boron content of the Ni–B alloy coating was measured by inductively coupled plasma spectroscopy (ICPS; ICPS-7500, Shimadzu Seisakusho). The phase transition behavior of the Ni–B alloy film was evaluated by differential scanning calorimetry (DSC; DSC8230SF, Rigaku). The amount of deposited Ni–B alloy was determined by weighing. For this, Ni–B alloy deposited VGCNFs were dried and weighed. The Ni–B alloy deposits were then dissolved in nitric acid. The VGCNFs in the nitric acid solution were filtered, dried, and weighed. The volume of the deposited Ni–B alloy was calculated by dividing the weight of the deposited Ni–B alloy by its density. The mean density was calculated based on the individual densities of nickel and boron. The mean thickness of the Ni–B alloy coating on the VGCNFs was roughly calculated by dividing the volume of the deposited Ni–B alloy by the surface area of the VGCNFs. The surface area of the VGCNFs was taken to be 13 $m^2 g^{-1}$.

3. Results and discussion

The electroless deposition behavior of Ni–B alloy on VGCNFs varied considerably with the bath pH. No deposits were observed on the VGCNFs at a pH of 4. At pH of 6 and 10, small amounts of inhomogeneous deposits were observed on the VGCNFs. Homogeneous deposition of Ni–B alloy on the VGCNFs was obtained at pH = 8. Fig. 1 shows an SEM image of Ni–B alloy-deposited VGCNFs fabricated using a plating bath containing 0.05 M DMAB at pH = 8. The reaction time was 600 s. Each VGCNF is homogeneously coated with the Ni–B alloy. Therefore, a bath pH of 8 was used in subsequent experiments in this study.

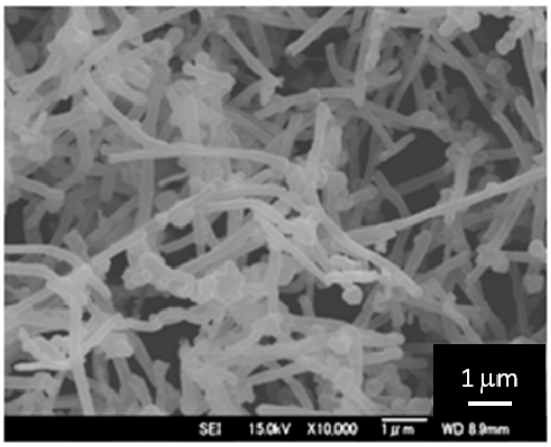

Fig. 1. SEM image of Ni–B alloy coated VGCNFs produced by electroless deposition at pH = 8. The DMAB concentration was 0.05 M and the reaction time was 600 s.

Fig. 2 shows the relationship between the DMAB concentration in the plating bath and the boron content in the Ni–B alloy deposits on the VGCNFs. The mean thickness of the Ni–B alloy deposits on the VGCNFs was ~100 nm. The boron content in the alloy deposits increased with increasing boron concentration in the plating bath, ranging from 14 to 24 atom% B (2.9 to 5.5 mass%). Thus, the composition of the Ni–B alloy deposits could be controlled by changing the

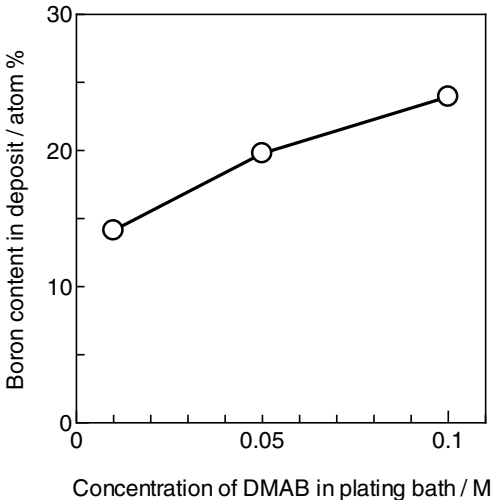

Fig. 2. Relationship between DMAB concentration in the plating bath and boron content in the deposits.

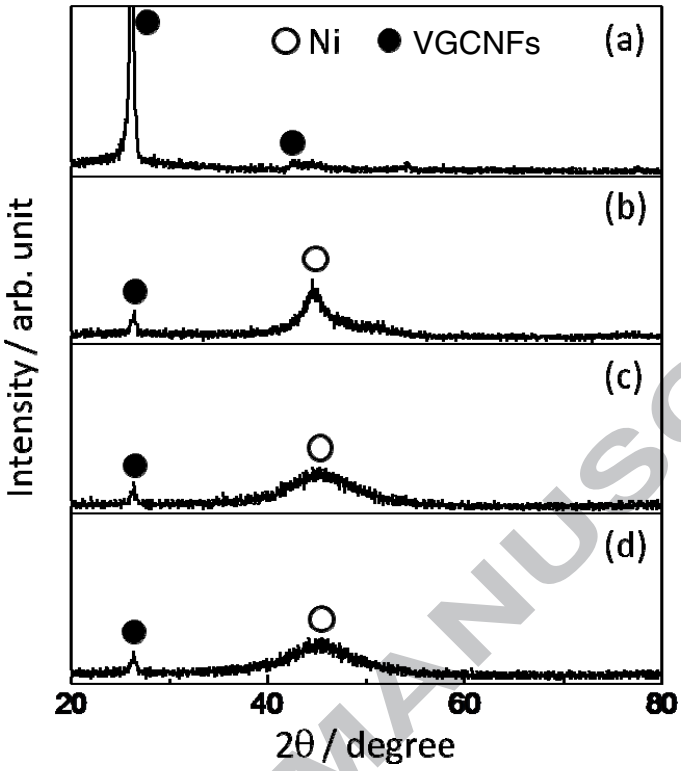

Fig. 3. XRD patterns of VGCNFs deposited with various compositions of Ni–B alloys; (a) VGCNFs before electroless deposition, (b) Ni–14 atom% B, (c) Ni–20 atom% B, and (d) Ni–24 atom% B.

DMAB concentration in the plating bath.

Fig. 3 shows XRD patterns of the Ni–B alloy-deposited VGCNFs fabricated using plating baths with various DMAB concentrations. For comparison, an XRD pattern for uncoated VGCNFs is also shown (Fig. 3a). A broad peak assigned to face-centered-cubic nickel and a sharp peak assigned to VGCNFs are observed at about 44 and 27°, respectively, in each pattern (Figs. 3b, c, and d). The sharpness of the peak assigned to face-centered-cubic nickel decreased with increasing boron content of the alloy deposits. Thus, the microstructure of the Ni–B alloy deposits on the VGCNFs changed from a semi-amorphous structure to an amorphous structure with increasing boron content in the alloy deposits.

Fig. 4 shows the relationship between the electroless deposition time (i.e., the reaction time) and the mean film thickness of the Ni–B alloy film on the VGCNFs. Two electroless plating baths with DMAB concentrations of 0.01 and 0.1 M were used. The mean film thickness increased proportionally with the reaction time. The film growth rate of the Ni–B alloy film from the plating bath with 0.1 M DMAB (Ni–24 atom% B) was about twice that of the Ni–B alloy film grown from the plating bath with 0.01 M DMAB (Ni–14 atom% B). Thus, the mean film thickness of the Ni–B alloy deposits on the VGCNFs can be controlled by varying the reaction time.

Figs. 5 and 6 show SEM images that reveal the growth of the Ni–B alloy films on the VGCNFs using plating baths with DMAB concentrations of 0.01 and 0.1 M, respectively. Fig. 5

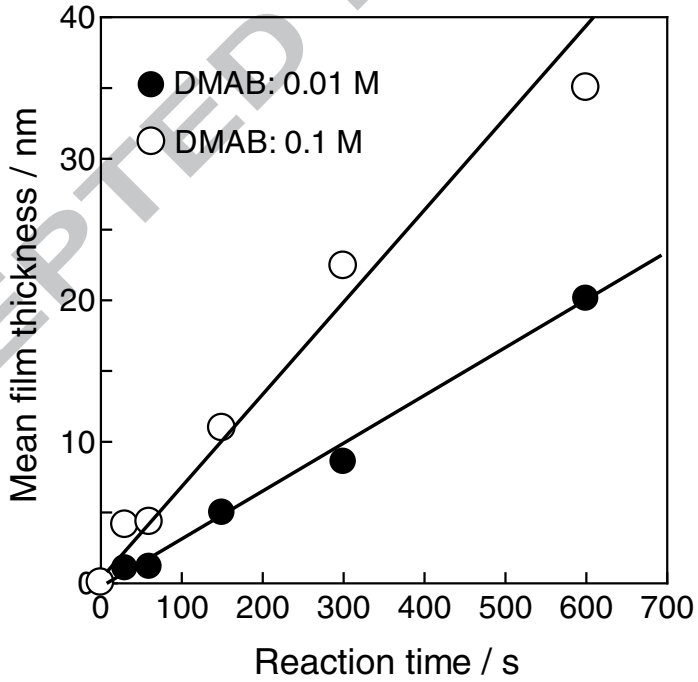

Fig. 4. Relationship between reaction time and mean film thickness of the Ni–B alloy on the VGCNFs.

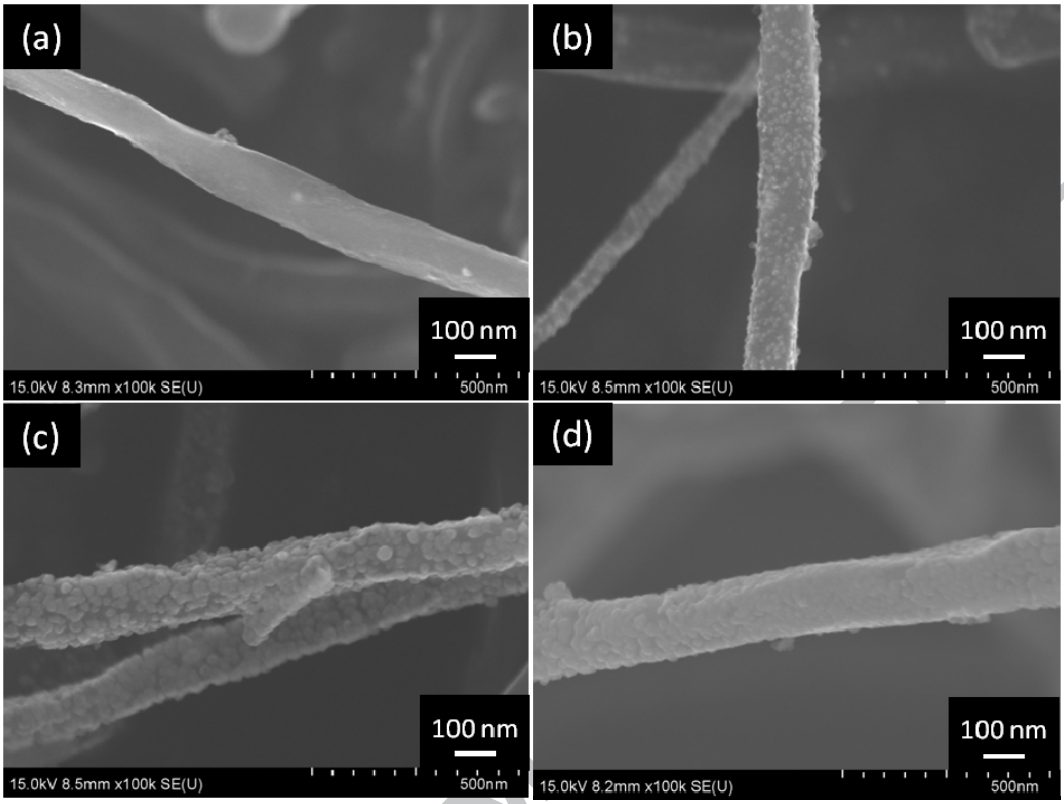

Fig. 5. SEM images showing the growth of Ni–B alloy deposits on VGCNFs using an electroless plating bath with 0.01 M DMAB (a) before electroless deposition and (b) after 30, (c) 150, and (d) 300 s.

shows the growth of the Ni–B alloy using the plating bath with 0.01 M DMAB. The Ni–B alloy (Ni–14 atom% B) thickness on the VGCNFs increased with increasing reaction time. Ni–B alloy particles are observed on the VGCNFs at 30 s (Fig. 5b). These particles grew on the VGCNFs (Fig. 5c) with increasing time and finally perfectly coated the VGCNFs at a reaction time of 300 s (Fig. 5d). This reaction time corresponds to a mean film thickness of about 10 nm (Fig. 4). After a reaction time of 300 s, the alloy films grew autocatalytically on the deposited Ni–B alloy on the VGCNFs. Thus, perfect coating of each VGCNF with semi-amorphous Ni–B alloy (Ni–14 atom% B) was achieved at film thicknesses above 10 nm using a plating bath with 0.01 M DMAB.

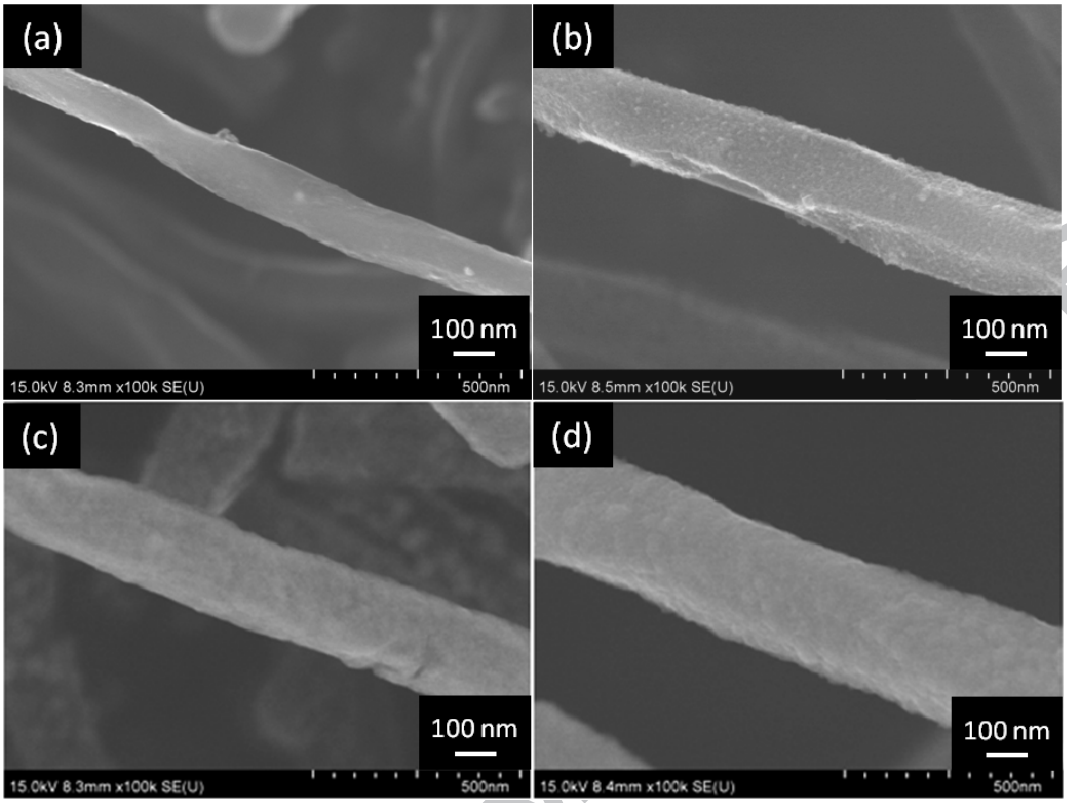

Fig. 6. SEM images showing growing process of Ni–B alloy deposits on VGCNFs from a plating bath with 0.1 M DMAB; (a) before electroless deposition, (b) 30, (c) 150, and (d) 300 s.

Fig. 6 shows the growth of the Ni–B alloy on the VGCNFs using the electroless plating bath with 0.1 M DMAB. The Ni–B alloy (Ni–24 atom% B) deposits grew on the VGCNFs with increasing reaction time. In contrast with Fig. 5, the VGCNFs in this case were coated perfectly even at a reaction time of 30 s (Fig. 6b), which corresponds to a film thickness of about 4 nm (Fig. 4). Subsequently, the alloy films grew autocatalytically on the deposited Ni–B alloy on the VGCNFs (Figs. 6c and d). The surface morphology was smoother than the Ni–14 atom% B alloy deposits.

Fig. 7 shows STEM images of the Ni–B alloy deposits on the VGCNFs from plating baths with DMAB concentrations of 0.01 and 0.1 M for a reaction time of 30 s. Fig. 7a and d show

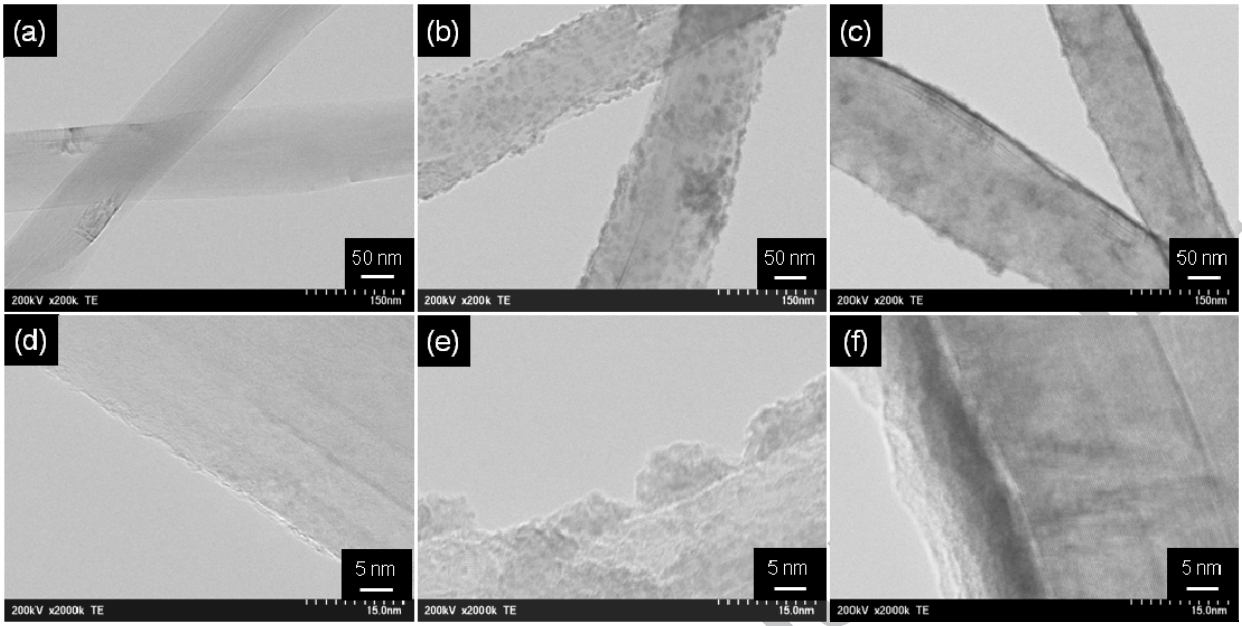

Fig. 7. STEM images of the Ni–B alloy deposits on VGCNFs from plating baths with different DMAB concentrations. (a) Before electroless deposition, (b) 0.01 M DMAB, (c) 0.1 M DMAB. (d)–(f) Show high magnification images of (a)–(c), respectively. Reaction time was 30 s.

STEM images of pristine VGCNFs (Fig. 7d: high magnification). A number of particles with diameters of several nanometers are visible on the VGCNFs from the plating bath with 0.01 M DMAB (Figs. 7b and e). Thus, the VGCNFs are not perfectly coated from the plating bath with 0.01 M DMAB. In contrast, VGCNFs were perfectly coated with Ni–B alloy films that are several nanometers thick from the plating bath with 0.1 M DMAB (Figs. 7c and f). This observed thickness is almost the same as the mean film thickness (Fig. 4). Therefore, each VGCNF was very uniformly coated with the Ni–B alloy film. This uniformity is an important advantage of electroless deposition.

Figs. 5, 6, and 7 demonstrate that it is possible to perfectly coat individual VGCNFs with a very thin Ni–B alloy film and that perfect coating of individual VGCNFs with an Ni–B alloy

film (Ni–24 atom% B alloy film) that is several nanometers thick is possible using a plating bath with 0.1 M DMAB.

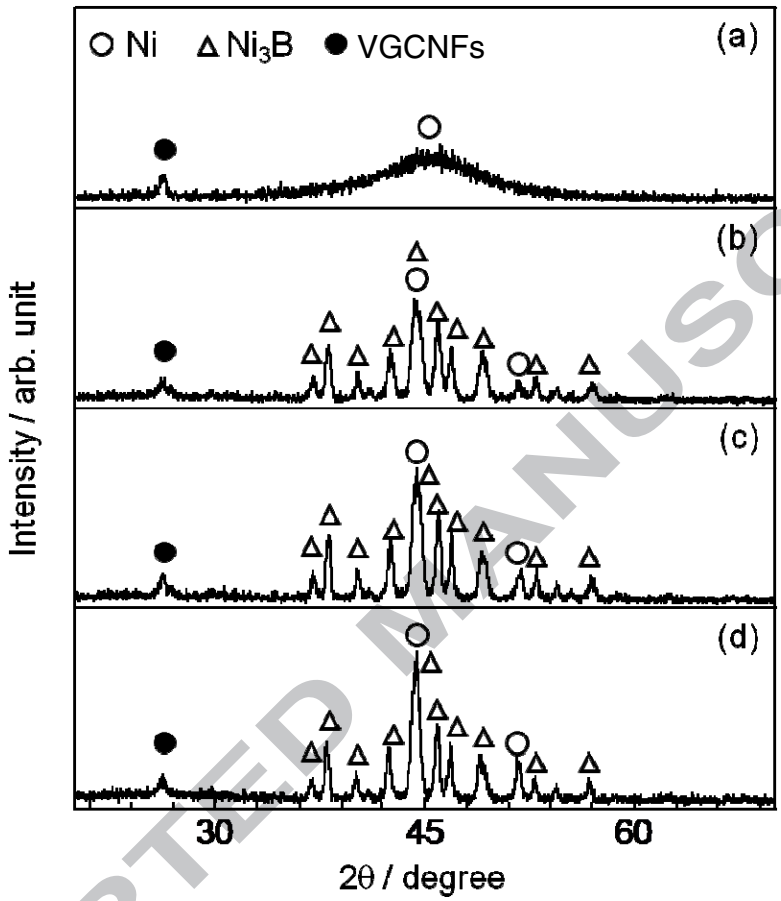

Fig. 8. XRD patterns of Ni–24 atom% B alloy coated VGCNFs after heat treatment at various temperatures. (a) Before heat treatment, (b) 300, (c) 400, and (d) 500°C. The alloy coatings were about 80 nm thick.

Fig. 8 shows XRD patterns of the Ni–24 atom% B alloy coated VGCNFs after heat treatment at various temperatures. For comparison, the XRD pattern of Ni–24 atom% B alloy coated VGCNFs before heat treatment is also shown (Fig. 8a). After heat treatment, sharp peaks assignable to the face-centered-cubic nickel phase and the Ni_3B phase were observed in all the XRD data (Figs. 8b, c and d). The sharpness of the peaks increased with increasing heat treatment temperature. According to the Ni–B binary alloy phase diagram [29], the Ni–24

atom% B alloy has stable phases consisting of face-centered-cubic nickel and Ni_3B between 700 and 1093°C. There was no data for stable phases of the Ni–B binary alloy below 700°C in the diagram. If the stable phases of the Ni–B alloy below 700°C are the same as those above 700°C, the Ni–24 atom% B alloy film will have stable phases after heat treatment.

A Ni–B alloy consisting of an amorphous phase is generally nonmagnetic; in contrast, the Ni–B alloy containing the face-centered-cubic nickel phase is ferromagnetic; the degree of ferromagnetism depends on the crystallinity. Thus, heat treatment converted the nonmagnetic Ni–24 atom% B alloy film with an amorphous phase on the VGCNFs into a ferromagnetic alloy film with stable crystalline phases consisting of face-centered-cubic nickel and Ni_3B. According to the Ni–C binary alloy phase diagram [29], graphite does not form a stable compound with nickel above 500°C, and it is estimated that graphite and nickel do not form a solid solution with each other and do not form any compound below 500°C. Therefore, the MWCNTs and the Ni–B alloy film did not form any stable compounds during heat treatment. SEM observations revealed no cracks or exfoliation of the Ni–B alloy films even after heat treatment. The Ni–14 atom% B alloy coated VGCNFs showed similar XRD patterns as those in Fig. 8 after heat treatment. The Ni–14 atom% B alloy coating also consisted of face-centered-cubic nickel and Ni_3B. The peak intensities of the face-centered-cubic nickel phase were higher and those of Ni_3B were lower than those of the Ni–24 atom% B alloy film. Furthermore, cracks and exfoliation were not observed even after heat treatment.

Fig. 9 shows DSC data for the Ni–24 atom% B alloy coated VGCNFs. An obvious endothermic peak is observed at about 300°C. Similar DSC results were reported for Ni–B alloy films on metal substrates [15,30] and an alumina substrate [22]. This endothermic peak is considered to be due to the phase transition from an amorphous phase of the Ni–B alloy to

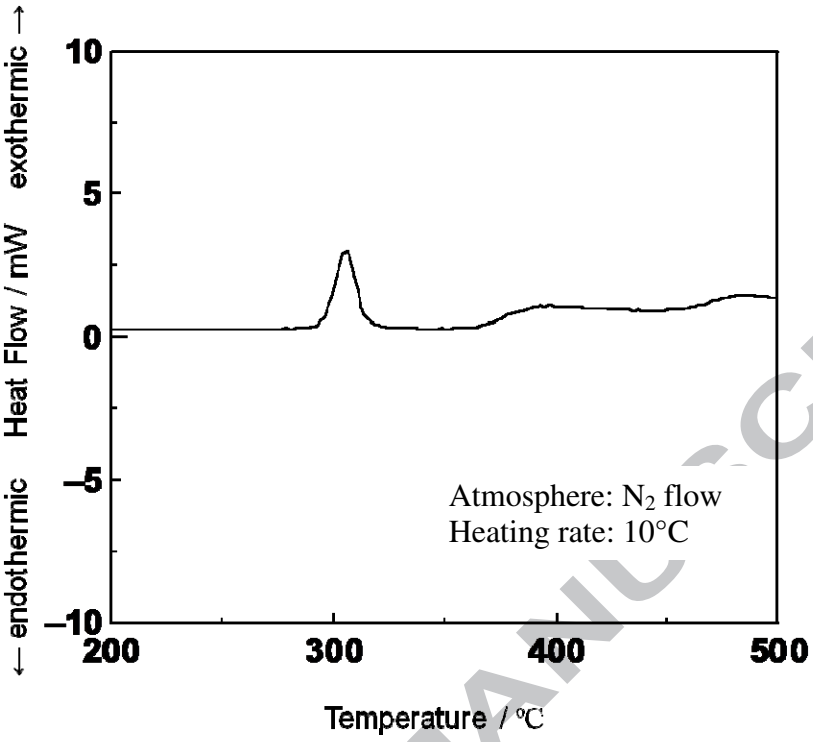

Fig. 9. DSC data for Ni–24 atom% B alloy coated VGCNFs.

crystalline phases consisting of face-centered-cubic nickel and Ni_3B [30]. These results are consistent with the XRD data after heat treatment (Fig. 8).

4. Conclusions

Electroless Ni–B alloy coated VGCNFs were successfully fabricated. The VGCNFs were perfectly coated with semi-amorphous Ni–B alloy (Ni–14 atom% B) with a thickness of about 10 nm and with amorphous phase Ni–B alloy (Ni–24 atom% B) with a thickness of several nanometers. The thickness of these Ni–B alloy coatings could be controlled by varying the reaction time. Heat treatment altered the phase structure of these coatings from metastable phases to stable crystalline phases consisting of face-centered-cubic nickel and Ni_3B. The coatings did not show any cracks or exfoliation even after heat treatment. These Ni–B coated VGCNFs are

anticipated to be used in various applications, such as raw materials for high strength metal/VGCNF composites and catalysts for hydrogenation of organic substances. Fabrication of amorphous phase Ni–B alloy particles with nanometer sizes on VGCNFs may enhance the catalytic properties for hydrogenation. We plan to do this in the future. This Ni–B alloy coating technology is expected to be applied to CNTs.

Acknowledgements

This research was supported by the Regional Innovation Cluster Program of Nagano granted by MEXT, Japan.

References

[1] Oberlin A, Endo M, Koyama T. Filamentous growth of carbon through benzene decomposition. J. Cryst. Growth 1976; 32:335–49.

[2] Iijima S, Ichihashi T. Single-shell carbon nanotubes of 1-nm diameter. Nature 1993; 363:603–5.

[3] Ma CCM, Huang YL, Kuan HC, Chiu YS. Preparation and electromagnetic interference shielding characteristics of novel carbon-nanotube/siloxane/poly(urea urethane) nanocomposites. J. Polym. Sci. Pol. Phys. 2005; 43:345–58.

[4] Jou WS, Cheng HZ, Hsu CF. A carbon nanotube polymer-based composite with high electromagnetic shielding. J. Electron. Mater. 2006; 35:462–70.

[5] Kim C, Kim YJ, Kim YA, Yanagisawa T, Park KC, Endo M. High performance of cup-stacked-type CNTs as a Pt–Ru catalyst support for fuel cell applications. J. Appl. Phys. 2004; 96:5903–5.

[6] Matsumoto T, Komatsu T, Nakano H, Arai K, Nagashima Y, Yoo E, et al. Efficient usage of highly-dispersed Pt on carbon nanotubes for electrode catalysts of polymer electrolyte fuel cells. Catal. Today 2004; 90:277–81.

[7] Li Q, Fan S, Han W, Sun C, Liang W. Coating of carbon nanotube with nickel by electroless plating method. Jpn. J. Appl. Phys. 1997;36:L501–3.

[8] Chen WX, Tu JP, Wang LY, Gan HY, Xu ZD, Zhang XB. Tribological application of carbon nanotubes in a metal-based composite coating and composites. Carbon 2003;41:215–22.

[9] Zhang HZ, Zhang XJ, Zhang YK. Structure and properties of electroless nickel–boron alloy. Plating Surf. Finish 1991; 80:80–4.

[10] Delaunois F, Petitjean JP, Lienard P, Jacob-Duliere M. Autocatalytic electroless nickel–boron plating on light alloys. Surf. Coat. Technol. 2000; 124:201–9.

[11] Delaunois F, Lienard P. Heat treatments for electroless nickel–boron plating on aluminum alloys. Surf. Coat. Technol. 2002; 160:239–48.

[12] Krishnaveni K, Sankara Narayanan TSN, Seshadri SK. Electroless Ni–B coatings: preparation and evaluation of hardness and wear resistance. Surf. Coat. Technol. 2005; 190:115–21.

[13] Ziyuan S, Deqing W, Zhimin D. Nanocrystalline Ni–B coating surface strengthening pure copper. Appl. Surf. Sci. 2006; 253:1051–4.

[14] Oraon B, Majumdar G, Ghosh B. Improving hardness of electroless Ni–B coatings using optimized deposition conditions and annealing. Mater Des 2008; 29:1412–8.

[15] Anik M, Korpe E, Sen E. Effect of coating bath composition on the properties of electroless nickel–boron films. Surf. Coat. Technol. 2008; 202:1718–27.

[16] Sawa Y, Yamashita K, Kitadani T, Noda D, Hattori T. Fabrication of high hardness Ni mold with electroless nickel–boron thin layer. Microsyst. Technol. 2010; 16:1369–75.

[17] Velez M, Quinones H, Di Giampaolo AR, Lira J, Grigorescu IC. Electroless Ni–B coated WC and VC powders as precursors for liquid phase sintering. Int. J. Refract. Met. Hard Met. 1999; 17:99–103.

[18] Zhu X, Dong H, Lu K. Coating different thickness nickel–boron nanolayers onto boron carbide particles. Surf. Coat. Technol. 2008; 202:2927–34.

[19] Dong H, Zhu X, Lu K. Morphology and composition of nickel–boron nanolayers coating on boron carbide particles. J. Mater. Sci. 2008; 43:4247–56.

[20] Wang L, Zhu X, Zhou J, Ouyang S. Morphology analysis of nickel–boron/diamond electroless deposition. J Wuhan Univ. Technol. Mater. Sci. Ed 2008; 23:169–72.

[21] Li X, Han X, Tan Y, Xu P. Preparation and microwave absorption properties of Ni–B alloy-coated Fe_3O_4 particles. J. Alloys Compd. 2008; 464:352–6.

[22] Xue D, Chen H, Wu GH, Deng JF. Amorphous Ni–B alloy membrane: preparation and application in ethanol dehydrogenation. Appl. Catal. A: Gen 2001; 214:87–94.

[23] Wu. Z, Zhang M, Ge S, Zhang Z, Li W, Tao K. Synthesis and characterization of a porous amorphous Ni–B catalyst on titania by silver-catalyzed electroless plating. J. Mater. Chem. 2005; 15:4928–33.

[24] Chen X, Yang W, Wang S, Qiao M, Yan S, Fan K, He H. Amorphous Ni–B hollow spheres synthesized by controlled organization of Ni–B nanoparticles over PS beads via surface seeding/electroless plating. New J. Chem. 2005; 29:266–8.

[25] Ge S, Wu Z, Zhang M, Li W, Tao K. Sulfolene hydrogenation over an amorphous Ni–B alloy catalyst on MgO. Ind. Eng. Chem. Res. 2006; 45:2229–34.

[26] Wu Z, Zhang M, Li W, Mu S, Tao K. Study on the deactivation of supported amorphous Ni–B catalyst in hydrogenation. J. Mol. Catal. A 2007; 273:277–83.

[27] Wu ZJ, Ge SH, Zhang MH, Li W, Mu SC, Tao KY. Controlled synthesis of supported nickel boride catalyst using electroless plating. J. Phys. Chem. 2007; 111:8587–93.

[28] Endo M. Grow carbon fibers in the vapor phase. CHEMTEC 1988; 18:568–76.

[29] Binary Alloy Phase Diagrams, 2nd ed., ASM International, Materials Park, OH, 1996.

[30] Narayanan TSNS, Seshadri SK. Formation and characterization of borohydride reduced electroless nickel deposits. J. Alloy Compd. 2004; 365:197–205.

Figure captions

Fig. 1. SEM image of Ni–B alloy coated VGCNFs produced by electroless deposition at pH = 8. The DMAB concentration was 0.05 M and the reaction time was 600 s.

Fig. 2. Relationship between DMAB concentration in the plating bath and boron content in the deposits.

Fig. 3. XRD patterns of VGCNFs deposited with various compositions of Ni–B alloys; (a) VGCNFs before electroless deposition, (b) Ni–14 atom% B, (c) Ni–20 atom% B, and (d) Ni–24 atom% B.

Fig. 4. Relationship between reaction time and mean film thickness of the Ni–B alloy on the VGCNFs.

Fig. 5. SEM images showing the growth of Ni–B alloy deposits on VGCNFs using an electroless plating bath with 0.01 M DMAB (a) before electroless deposition and (b) after 30, (c) 150, and (d) 300 s.

Fig. 6. SEM images showing growing process of Ni–B alloy deposits on VGCNFs from a plating bath with 0.1 M DMAB; (a) before electroless deposition, (b) 30, (c) 150, and (d) 300 s.

Fig. 7. STEM images of the Ni–B alloy deposits on VGCNFs from plating baths with different DMAB concentrations. (a) Before electroless deposition, (b) 0.01 M DMAB, (c) 0.1 M DMAB. (d)–(f) Show high magnification images of (a)–(c), respectively. Reaction time was 30 s.

Fig. 8. XRD patterns of Ni–24 atom% B alloy coated VGCNFs after heat treatment at various temperatures. (a) Before heat treatment, (b) 300, (c) 400, and (d) 500°C. The alloy coatings were about 80 nm thick.

Fig. 9. DSC data for Ni–24 atom% B alloy coated VGCNFs.